Bayesian Inversion in Resin Transfer Moulding

Michael Causon

University of Nottingham

Joint work with: M. Tretyakov, M. Iglesias, A. Endruweit, M. Matveev

UCL
May 21, 2023

Overview

1. Resin Transfer Moulding (RTM)
2. The 1D Forward Problem
3. The Inverse Problem
4. Results
5. Conclusion

Resin Transfer Moulding (RTM)

Uses of RTM: aerospace, automotive and marine industries.
Features: lightweight, high relative strength, form complex shapes, durable.

Figure: (Left to right, top to bottom) Composition of Boeing 787 [1], Formula 1 car [2], rowing boat [3], boat propeller [4], wind turbine rotator blade [5], car wing mirror [6].

The RTM Process

RTM uses 2 materials: a fibre-reinforced preform and liquid resin.

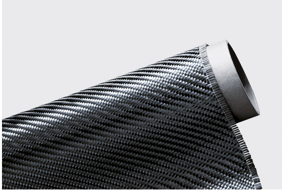

Figure: (a) Carbon fibre preform [7]

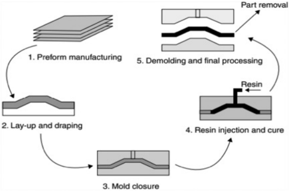

Figure: (b) RTM schematic [8]

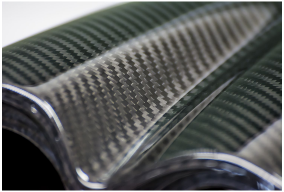

Figure: (c) Finished composite part [9]

The RTM Process

RTM uses 2 materials: a fibre-reinforced preform and liquid resin.

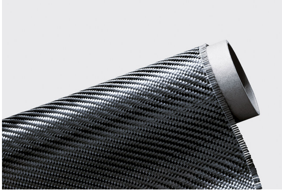

Figure: (a) Carbon fibre preform [7]

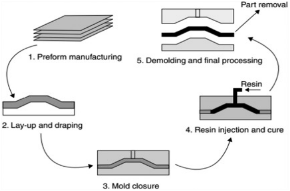

Figure: (b) RTM schematic [8]

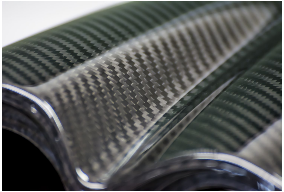

Figure: (c) Finished composite part [9]

Motivation

Variations in permeability

⇓

Inhomogeneous resin flow

⇓

Variations in mechanical properties of part

⇓

Part discarded upon testing

Aims

Inverse problem: find (log-)permeability using pressure data recorded during injection to:

1. aid non-destructive evaluation
2. support the use of active control RTM

We emphasize the importance of **speed**.

Overview

1. Resin Transfer Moulding (RTM)
2. The 1D Forward Problem
3. The Inverse Problem
4. Results
5. Conclusion

Darcy Flow in 1D

Solution in 1D [10, 11, 12]

Let $u \in X \equiv L^2([0, D^*])$. Define $F_u(x) := \int_0^x e^{-u(z)} dz$ and $W_u(x) := \int_0^x F_u(\xi) d\xi$.

$$\Upsilon_u(t) = W_u^{-1}\left(\frac{p_I - p_0}{\mu\phi} t\right), \tag{1}$$

$$p_u(x,t) = \begin{cases} p_I - (p_I - p_0)\frac{F_u(x)}{F_u(\Upsilon_u(t))}, & x \in [0, \Upsilon_u(t)), \\ p_0, & x \in [\Upsilon_u(t), D^*]. \end{cases} \tag{2}$$

Fréchet derivative of the forward problem

For $0 \leq x \leq \Upsilon(t)$, the Frechet derivative of (Υ, p) w.r.t u is given by:

$$D\Upsilon_u(t)h = \frac{\int_0^{\Upsilon(t)} \int_0^{\xi} e^{-u(z)} h(z) dz d\xi}{F_u(\Upsilon(t))}, \tag{3}$$

$$Dp_u(x,t)h = \frac{(p_I - p_0)}{F_u(\Upsilon(t))^2}\Big[F_u(\Upsilon(t)) \int_0^x e^{-u(z)} h(z) dz - F_u(x) \int_0^{\Upsilon(t)} e^{-u(z)} h(z) dz + F_u(x) e^{-u(\Upsilon(t))} D\Upsilon_u(t)h\Big]. \tag{4}$$

The Forward Map

At N times $0 < t_1 < \ldots < t_N < \tau^*$, suppose M sensors are used to record resin pressure. Let $Y \equiv \mathbb{R}^{NM}$. Define the **forward map** $\mathcal{G} : (X, \langle\cdot,\cdot\rangle_X) \to (Y, \langle\cdot,\cdot\rangle_Y)$ by

$$\mathcal{G}(u) = \left[\left\{ p_u(x_m, t_1) \right\}_{m=1}^{M}, \ldots, \left\{ p_u(x_m, t_N) \right\}_{m=1}^{M} \right]^T, \quad u \in X. \tag{5}$$

Example: let $M = N = 5$.

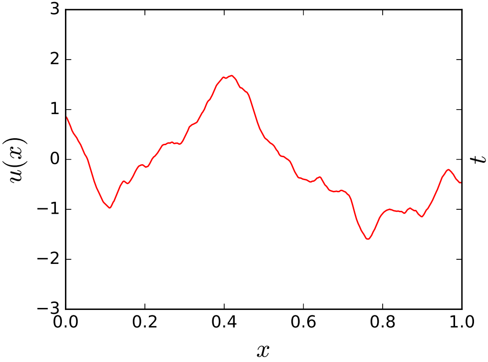

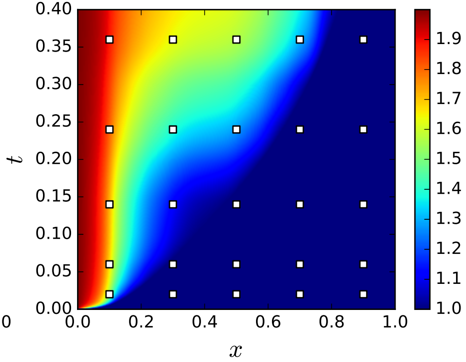

Figure: The forward problem and the forward map

Overview

1. Resin Transfer Moulding (RTM)
2. The 1D Forward Problem
3. The Inverse Problem
4. Results
5. Conclusion

The Inverse Problem

Estimate $u \in X$ in the expression

$$y = \mathcal{G}(u) + \eta, \tag{6}$$

where

- $\mathcal{G} : (X, \langle \cdot, \cdot \rangle_X) \to (Y, \langle \cdot, \cdot \rangle_Y)$ is the forward map
- $y \in Y$ are measurements of the system
- $\eta \in Y$ is random measurement noise

The Bayesian approach

Assume that both u and η are Gaussian random variables/fields:

1. $u \sim N(\bar{u}, \mathcal{C})$, where $\mathcal{C}$ arises from the Matérn [14] covariance function
2. $\eta \sim N(0, \Sigma) \implies y|u \sim N(\mathcal{G}(u), \Sigma)$, where Σ is given and diagonal

Using Bayes' rule $\mathbb{P}(u|y) \propto \mathbb{P}(u)\mathbb{P}(y|u)$, the posterior is given by

$$\mathbb{P}(u|y) \propto \exp\left(-\frac{1}{2}\left\|\Sigma^{-1/2}(y - \mathcal{G}(u))\right\|_Y^2 - \frac{1}{2}\left\|\mathcal{C}^{-1/2}(u - \bar{u})\right\|_X^2 \right). \tag{7}$$

Sampling from the Posterior

Case study: $\mathcal{G}$ is linear, i.e. $\mathcal{G}(u) = \mathcal{G}u$

Recall $u \sim N(\bar{u}, \mathcal{C})$ and $\eta \sim N(0, \Sigma)$. The posterior is Gaussian $u|y \sim N(\hat{u}, \hat{\mathcal{C}})$ with

$$\hat{u} = \bar{u} + \mathcal{C}\mathcal{G}^* \left[\mathcal{G}\mathcal{C}\mathcal{G}^* + \Sigma\right]^{-1} (y - \mathcal{G}\bar{u}), \tag{8}$$

$$\hat{\mathcal{C}} = \mathcal{C} - \mathcal{C}\mathcal{G}^* \left[\mathcal{G}\mathcal{C}\mathcal{G}^* + \Sigma\right]^{-1} \mathcal{G}\mathcal{C} \tag{9}$$

Case study: $\mathcal{G}$ is non-linear

No such solution exists. We must use Markov chain Monte Carlo (MCMC) methods.

Linearisation around the maximum a-posteriori (LMAP) estimate

Suppose $\mathcal{G}(u) \approx \mathcal{G}(u_{map}) + D\mathcal{G}(u_{map})(u - u_{map})$. Approximate $u \approx N(u_{map}, \mathcal{C}_{map})$ with

$$u_{map} = \underset{u \in X}{\operatorname{argmin}} \frac{1}{2} \left\| \Sigma^{-1/2}(y - \mathcal{G}(u)) \right\|_Y^2 + \frac{1}{2} \left\| \mathcal{C}^{-1/2}(u - \bar{u}) \right\|_X^2, \tag{10}$$

$$\mathcal{C}_{map} = \mathcal{C} - \mathcal{C} D\mathcal{G}^*(u_{map}) \left[D\mathcal{G}(u_{map}) \mathcal{C} D\mathcal{G}^*(u_{map}) + \Sigma \right]^{-1} D\mathcal{G}(u_{map}) \mathcal{C}. \tag{11}$$

Linearisation around the maximum a-posteriori (LMAP) estimate

For non-linear $\mathcal{G}$, the approximate posterior is $u|y \approx N(u_{map}, \mathcal{C}_{map})$ where

$$u_{map} = \underset{u \in X}{\operatorname{argmin}} \frac{1}{2} \left\| \Sigma^{-1/2}(y - \mathcal{G}(u)) \right\|_Y^2 + \frac{1}{2} \left\| \mathcal{C}^{-1/2}(u - \bar{u}) \right\|_X^2, \tag{12}$$

$$\mathcal{C}_{map} = \mathcal{C} - \mathcal{C} D\mathcal{G}^*(u_{map}) \left[D\mathcal{G}(u_{map}) \mathcal{C} D\mathcal{G}^*(u_{map}) + \Sigma \right]^{-1} D\mathcal{G}(u_{map}) \mathcal{C}. \tag{13}$$

Here, $D\mathcal{G}^*(u) : Y \to X$ is the adjoint of $D\mathcal{G}(u) : X \to Y$ defined by

$$\langle D\mathcal{G}(u)h, v \rangle_Y = \langle h, D\mathcal{G}^*(u)v \rangle_X, \quad \forall h \in X,\ v \in Y. \tag{14}$$

Levenberg-Marquardt algorithm ($u \to u_{map}$)

Define $A_k := D\mathcal{G}(u_k)$ and $A_k^* := D\mathcal{G}^*(u_k)$. Let $u_0 = \bar{u}$ and $\alpha_k \to 0$ according to [19].

$$u_{k+1} = u_k + \frac{\bar{u} - u_k}{1 + \alpha_k} + \mathcal{C} A_k^* \left[A_k \mathcal{C} A_k^* + (1 + \alpha_k)\Sigma \right]^{-1} \left(y - \mathcal{G}(u_k) - \frac{A_k(\bar{u} - u_k)}{1 + \alpha_k} \right). \tag{15}$$

The Adjoint

Note $D\mathcal{G}(u)h = \left[\{Dp_u(x_m, t_1)h\}_{m=1}^{M}, ..., \{Dp_u(x_m, t_N)h\}_{m=1}^{M}\right]^T$.

Riesz Representation Theorem [20]

Since $D\mathcal{G}(u) : X \to Y$ is linear and bounded, then $\exists R_m^n(u) \in X$ such that $\forall h \in X$

$$[D\mathcal{G}(u)h]_i = Dp(x_m, t_n)h = \langle \mathcal{C}^{-1/2} R_m^n(u), \mathcal{C}^{-1/2} h \rangle_X. \quad (16)$$

The Representers

The representers are given by $R_m^n = H(\Upsilon(t_n) - x_m)\mathcal{C}Q_m^n$ where

$$Q_m^n[u](x) = \frac{(p_l - p_0)}{F_u(\Upsilon(t_n))^2}\Big[F_u(\Upsilon(t_n))H(x_m - x)e^{-u(x)} - F_u(x_m)H(\Upsilon(t_n) - x)e^{-u(x)} + \frac{F_u(x_m)}{F_u(\Upsilon(t_n))}e^{-u(\Upsilon(t_n))}e^{-u(x)}\max\{\Upsilon(t_n) - x, 0\}\Big]. \quad (17)$$

One can show that

1. $\mathcal{C}D\mathcal{G}^*(u) = [\{R_m^1\}_{m=1}^M, ..., \{R_m^N\}_{m=1}^M] := \mathbf{R}(u)$
2. Let $\mathcal{R}(u) := D\mathcal{G}(u)\mathcal{C}D\mathcal{G}^*(u)$. Then $[\mathcal{R}(u)]_{ij} = \left\langle \mathcal{C}^{-1/2}[\mathbf{R}(u)]_i, \mathcal{C}^{-1/2}[\mathbf{R}(u)]_j \right\rangle_X$

Overview

1. Resin Transfer Moulding (RTM)
2. The 1D Forward Problem
3. The Inverse Problem
4. Results
5. Conclusion

Experimental Setup

Physical conditions

Constants: $p_l = 2$, $p_0 = 1$, $D^* = 1$,
Observation times: $(t_1, t_2, t_3, t_4, t_5) = (0.02, 0.06, 0.14, 0.24, 0.36)$.

The Prior

$u \sim N(0, \mathcal{C})$ where $\mathcal{C}h = \int_0^{D^*} c(x, x')h(x')dx'$ with

$$c(x, x') = \sigma^2 \frac{2^{1-\nu}}{\Gamma(\nu)} \left(\frac{|x - x'|}{l} \right)^{\nu} K_{\nu} \left(\frac{|x - x'|}{l} \right), \quad \sigma^2 = 0.5, \quad l = 0.1, \quad \nu = 1.5. \tag{18}$$

The Data

Assume that $u_{true} \sim \mathbb{P}(u)$ and that data are generated by

$$y = \mathcal{G}(u_{true}) + N(0, \Sigma), \tag{19}$$

where $\Sigma_{ii} = (0.01[\mathcal{G}(u_{true})]_i)^2$, i.e. 1% of noise-free observations.

Example of LMAP

Define $\mu_i = \mathbb{P}(u|y^{(i)})$, where $y^{(i)}$ is all data collected up to time t_i.

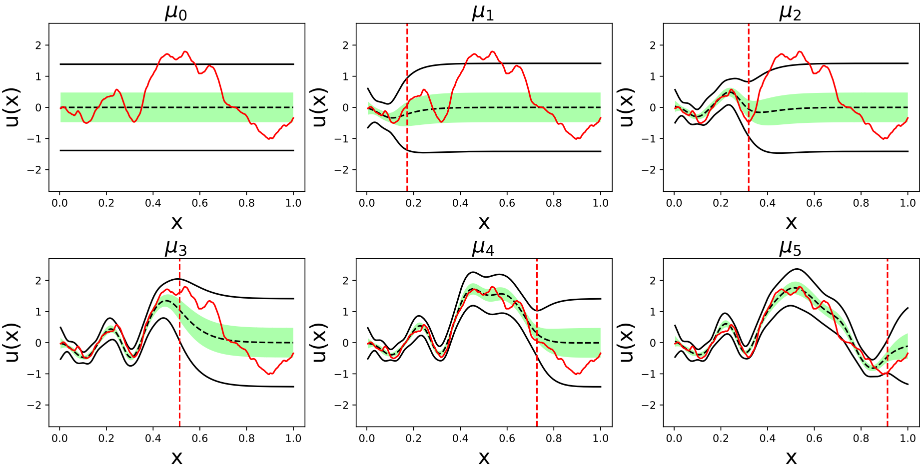

Figure: Domain equipped with $M = 15$ sensors. True permeability and true front location in red. Posterior mean is dashed black, along with 50% and 95% uncertainty bands.

Comparison

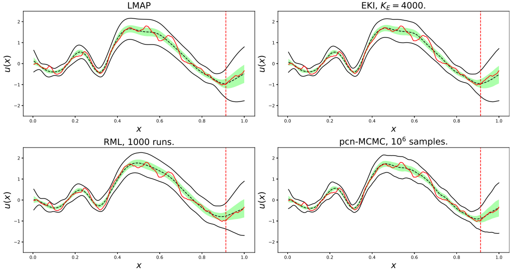

Define relative error by:

$$\mathbf{E}_5^{(\cdot)} = \frac{\|\bar{u}_5^{(\cdot)} - \bar{u}_5^{MCMC}\|_X}{\|\bar{u}_5^{MCMC}\|_X}, \quad \mathbf{S}_5^{(\cdot)} = \frac{\|\sigma_5^{(\cdot)} - \sigma_5^{MCMC}\|_X}{\|\sigma_5^{MCMC}\|_X}. \tag{20}$$

Algorithm	$\mathbf{E}_5^{(\cdot)}$	$\mathbf{S}_5^{(\cdot)}$	Multiprocessing	Computation time
pcn-MCMC	-	-	✘	9.186 hrs
EKI	0.06199	**0.09017**	✓	22.29 mins
RML	0.08621	0.2146	✓	30.10 mins
LMAP	**0.05366**	0.1774	✘	**7.240 secs**

Table: Results for each method.

Overview

1. Resin Transfer Moulding (RTM)
2. The 1D Forward Problem
3. The Inverse Problem
4. Results
5. Conclusion

- # Conclusion
  - LMAP is extremely fast, but requires thorough knowledge of $\mathcal{G}$ and $D\mathcal{G}$
  - Gaussian approximations are reasonably accurate
  - Representer theory helped to find the adjoint $D\mathcal{G}^*$
- # Further work
  - Addressing the inverse problem when no analytical solution exists
  - Replacing $\mathcal{G}$ with surrogate models
  - Apply LMAP methodology to 2D problem

Acknowledgements
This work was supported by the Engineering and Physical Sciences Research Council, UK [grant number EP/P006701/1]; through the EPSRC Future Composites Manufacturing Research Hub.

References

[1] Boeing (2006)
Boeing 787 from the ground up
AERO Q4, 17 – 23.

[2] Formula 1 (2023)
FIRST LOOK: Alfa Romeo show off 2023 C43 F1 car with striking new livery

[3] SL Racing (2021)
Built to win
Quality in every detail

[4] Fiberdyne (2019)
Carbon fiber marine propeller

[5] Composites World (2021)
Customized resin flow mesh products save time, cost for wind turbine blade manufacturers

[6] Composites World (2019)
Would you like carbon fiber with that car?

[7] SGL Carbon (2023)
SIGRATEX® non-crimp fabrics, woven fabrics, non-wovens, and stacks
The Drapables

[8] E. Sozer, P. Simacek, and S. Advani (2012)
Resin transfer molding (RTM) in polymer matrix composites
Manufacturing techniques for polymer matrix composites (PMCs), 245 – 309
Woodhead Publishing

References (cont.)

[9] ThoughCo. (2019)
Science
Carbon Fiber Manufacturing Companies

[10] M. Park, and M.V. Tretyakov (2017)
Stochastic resin transfer molding process
SIAM/ASA Journal on Uncertainty Quantification 5.1, 1110 – 1135

[11] D.M. Tartakovsky and C.L. Winter (2001)
Dynamics of free surfaces in random porous media
SIAM Journal on Applied Mathematics 61, 1857 – 1876

[12] S.G. Advani and E.M. Sozer (2011)
Process modeling in composites manufacturing
CRC Press

[13] M. Fréchet (1911)
Sur la notion de différentielle
Comptes rendus de l'Académie des Sciences, 845 – 847

[14] B. Matérn (1986)
Spatial variation, vol. 36
Springer

[15] M. Iglesias, K. Law, and A. Stuart (2013)
Evaluation of Gaussian approximations for data assimilation in reservoir models
Computational Geosciences, 17, 851 – 885

References (cont.)

[16] S. Cotter, G. Roberts, A. Stuart, and D. White (2013)
MCMC methods for functions: modifying old algorithms to make them faster
Statistical Science, 28, 424 – 446

[17] M. Iglesias, M. Park, and M. V. Tretyakov (2018)
Bayesian inversion in resin transfer molding
Inverse Problems, 34, 424 – 446

[18] M. Matveev, A. Endruweit, A. Long, M. Iglesias, and M. Tretyakov (2021)
Bayesian inversion algorithm for estimating local variations in permeability and porosity of reinforcements using experimental data
Composites Part A: Applied Science and Manufacturing, 143

[19] A. Reynolds, D. Oliver, and N. Liu (2008)
Inverse theory for petroleum reservoir characterization and history matching
Cambridge University Press, 1 ed.

[20] K. Bryan (2008)
The Riesz representation theorem
Mathematical Analysis - The Johns Hopkins University

[21] M. Iglesias and Y. Yang (2021)
Adaptive regularisation for ensemble Kalman inversion
Inverse Problems 37.2

Sensor Density

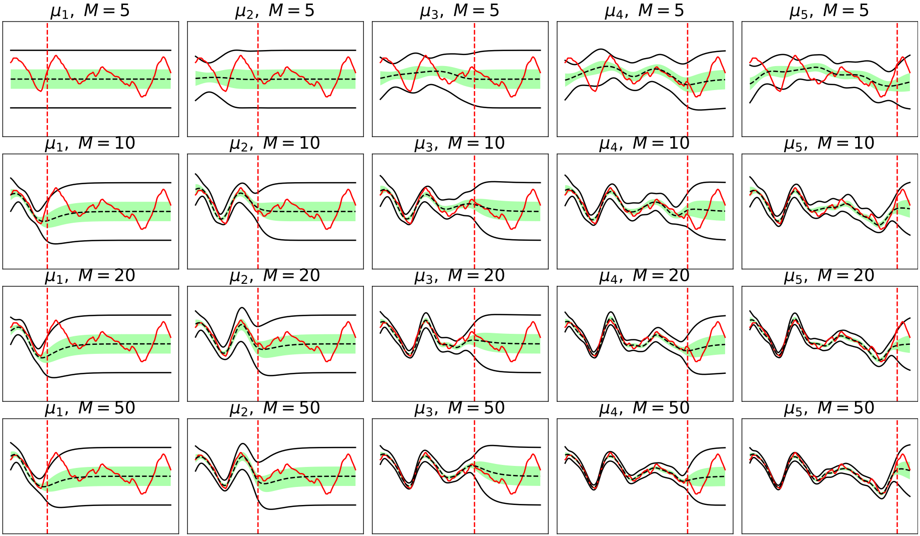

Figure: LMAP algorithm for various sensor densities. Here, $\mu_i = \mathbb{P}(u|y_1, \ldots, y_i)$

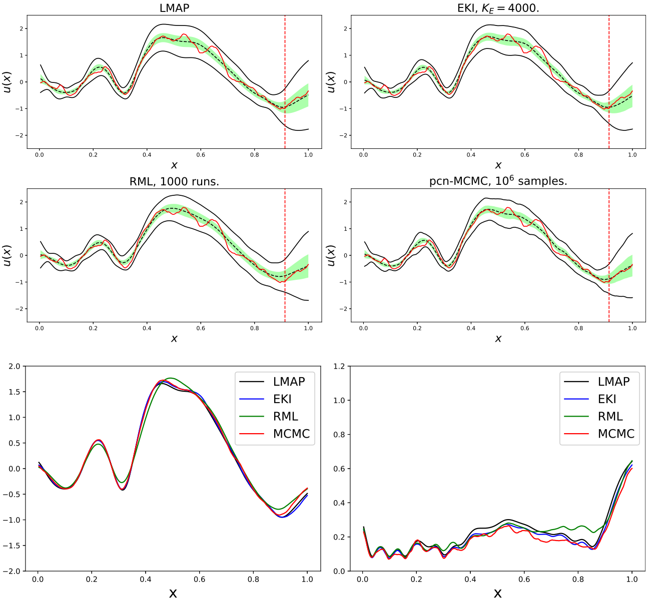
LMAP
EKI, $K_E = 4000$.
RML, 1000 runs.
pcn-MCMC, 10^6 samples.
u(x)
x
LMAP
EKI
RML
MCMC

Levenberg-Marquardt

We have a (non-linear) optimisation problem of the form

$$u_{map} = \underset{u \in X}{\operatorname{argmin}} \frac{1}{2} \left\| \Sigma^{-1/2} (y - \mathcal{G}(u)) \right\|_Y^2 + \frac{1}{2} \left\| \mathcal{C}^{-1/2} (u - \bar{u}) \right\|_X^2. \tag{21}$$

By considering some u_k in the neighbourhood of u,

1. linearise the forward map $\mathcal{G}(u) = \mathcal{G}(u_k) + D\mathcal{G}(u_k)(u - u_k)$
2. add further regularisation $R_k(u) = \frac{\alpha_k}{2} \|\mathcal{C}^{-1/2}(u - u_k)\|_X^2$

The (now) quadratic problem has iterative solution:

Levenberg-Marquardt algorithm

$$u_{k+1} = u_k + \frac{\bar{u} - u_k}{1 + \alpha_k} + h, \tag{22}$$

$$h = \mathcal{C} D\mathcal{G}^*(u_k) \left[D\mathcal{G}(u_k) \mathcal{C} D\mathcal{G}^*(u_k) + (1 + \alpha_k)\Sigma \right]^{-1} \left(y - \mathcal{G}(u_k) - \frac{D\mathcal{G}(u_k)(\bar{u} - u_k)}{1 + \alpha_k} \right).$$

where $u_0 = \bar{u}$ and $\alpha_k \to 0$ according to [19].

Further work details

Constrain the (regularised) optimisation problem with the forward problem:

$$\mathcal{L} = \frac{1}{2}\left\|\Sigma^{-1/2}(y - \mathcal{G}(u))\right\|_Y^2 + \frac{1}{2}\left\|\mathcal{C}^{-1/2}(u - \bar{u})\right\|_X^2 + \frac{\alpha_k}{2}\left\|\mathcal{C}^{-1/2}(u - u_k)\right\|_X^2 \tag{23}$$

$$- \int_0^T \int_0^{\Upsilon(t)} \frac{d}{dx}\left[e^{u(x)}\frac{dp}{dx}(x,t)\right]\lambda(x,t)dxdt + \int_0^T [p(0,t) - p_I]\alpha_1(t)dt \tag{24}$$

$$+ \int_0^T \left[\frac{d\Upsilon}{dt}(t) + \frac{1}{\mu\phi}e^{u(\Upsilon(t))}\frac{dp}{dx}(\Upsilon(t),t)\right]\kappa(t)dt + \int_0^T [p(\Upsilon(t),t) - p_0]\alpha_2(t)dt \tag{25}$$

$$+ \int_0^L [p(x,0) - p_0]\alpha_3(x)dx. \tag{26}$$

Linearise the non-linear terms and take derivatives in each direction to get

1. a set of state equations for $(D\Upsilon(t)h, Dp(x,t)h)$
2. a set of adjoint equations for (κ, λ)
3. an update equation for $u_k \to u_{k+1}$ which relies on the solutions to the above equations

Upon admitting the analytical solution at the last step, the update for $u_k \to u_{k+1}$ leads to the exact Levenberg-Marquardt algorithm on slide 12.

Algorithms

Algorithm 1 (pCN-MCMC) *Take* $u^{(0)} \sim N(\bar{u}, C), n = 1$, *and* $\beta \in (0,1)$. *Then,*

(1) pcN proposal. Generate u from

$$u = \sqrt{1-\beta^2} u^{(n)} + (1 - \sqrt{1-\beta^2})\bar{u} + \beta\xi, \qquad \text{with } \xi \sim N(0, C) \tag{22}$$

(2) Set $u^{n+1} = u$ *with probability* $a(u^n, u)$ *and* $u^{n+1} = u^n$ *with probability* $1 - a(u^n, u)$, *where*

$$a(u,v) = \min\left\{1, \exp\left(\Phi(u,y) - \Phi(v,y)\right)\right\} \tag{23}$$

(3) $n \mapsto n+1$ *and repeat.*

Figure: pcn-MCMC algorithm [15, 16]

Algorithm 3 (RML) *For* $j \in \{1, \ldots, N_e\}$

(1) Generate $u^{(j)} \sim N(\bar{u}, C)$
(2) Define $y^{(j)} = y + \eta^{(j)}$ *with* $\eta^{(j)} \sim N(0, \Gamma)$.
(3) Compute

$$u^{(j)}_{RML} = \text{argmin}_u \left\{ \Phi(u, y^{(j)}) + \frac{1}{2} ||u - u^{(j)}||^2_C \right\}. \tag{27}$$

Figure: RML algorithm [15]

Algorithm 1. Generic EKI (with perturbed observations).

Input:

1) $\{u_0^{(j)}\}_{j=1}^J$: Initial ensemble of inputs.
2) Measurements y and covariance of measurement errors Γ.

Set $\{u_n^{(j)}\}_{j=1}^J = \{u_0^{(j)}\}_{j=1}^J$ and $\theta = 0$
while $\theta < 1$ **do**

(1) Compute $\mathcal{G}_n^{(j)} = \mathcal{G}(u_n^{(j)}), \qquad j \in \{1, \ldots, J\}$

(2) Compute regularisation parameter α_n and check for convergence criteria
if converged **then**
set $\theta = 1$ and $n^* = n$

(3) Update each ensemble member

$$u_{n+1}^{(j)} = u_n^{(j)} + \mathcal{C}_n^{u\mathcal{G}}(\mathcal{C}_n^{\mathcal{G}\mathcal{G}} + \alpha_n \Gamma)^{-1}(y + \sqrt{\alpha_n}\xi_n - \mathcal{G}_n^{(j)}), \qquad j \in \{1, \ldots, J\}$$

where

$$C_n^{\mathcal{G}\mathcal{G}} \equiv \frac{1}{J-1}\sum_{j=1}^{J}(\mathcal{G}_n^{(j)} - \overline{\mathcal{G}}_n) \otimes (\mathcal{G}_n^{(j)} - \overline{\mathcal{G}}_n) \tag{16}$$

$$C_n^{u\mathcal{G}} \equiv \frac{1}{J-1}\sum_{j=1}^{J}(u_n^{(j)} - \overline{u}_n) \otimes (\mathcal{G}_n^{(j)} - \overline{\mathcal{G}}_n) \tag{17}$$

with $\overline{u}_n \equiv \frac{1}{J}\sum_{j=1}^J u_n^{(j)}$ and $\overline{\mathcal{G}}_n \equiv \frac{1}{J}\sum_{j=1}^J \mathcal{G}_n^{(j)}$.

$n \leftarrow n+1$
end
output: $\{u_{n^*}^{(j)}\}_{j=1}^J$ converged ensemble

Figure: EKI algorithm [21]

2D Problem

The forward problem for the pressure of resin $p(t,x)$ consists of the conservation of mass

$$\nabla \cdot \mathbf{v} = 0, \quad x \in D(t),\ t > 0, \tag{1}$$

where the flux $\mathbf{v}(x,t)$ is given by Darcy's law

$$\mathbf{v}(x,t) = -\frac{\kappa(x)}{\mu} \nabla p(x,t) \tag{2}$$

with the following initial and boundary conditions

$$p(x,t) = p_I,\ x \in \partial D_I,\ t \geqslant 0, \tag{3}$$

$$\nabla p(x,t) \cdot \mathbf{n}(x) = 0,\ x \in \partial D_N,\ t \geqslant 0, \tag{4}$$

$$V(x,t) = -\frac{\kappa(x)}{\mu\varphi} \nabla p(x,t) \cdot \mathbf{n}(x,t),\ x \in \Upsilon(t),\ t \geqslant 0, \tag{5}$$

$$p(x,t) = p_0,\ x \in \Upsilon(t),\ t > 0, \tag{6}$$

$$p(x,t) = p_0, x \in \partial D_O,\ t > 0, \tag{7}$$

$$p(x,0) = p_0,\ x \in D^*, \tag{8}$$

$$\Upsilon(0) = \partial D_I. \tag{9}$$

Figure: 2D forward problem [17]